Title: Hot pressed K0.5Na0.5nbo3 material for piezoelectric transformer for energy harvesting

Author: Lucjan Kozielski, Kamil Feliksik, Beata Wodecka-Duś; Diana Szalbot, S. Tutu

L. KOZIELSKI*#, K. FELIKSIK*, B. WODECKA-DUŚ*, D. SZALBOT*, S. TUTU**

HOT PRESSED K$_{0.5}$Na$_{0.5}$NbO$_3$ MATERIAL FOR PIEZOELECTRIC TRANSFORMER FOR ENERGY HARVESTING

An optimized method of vibration Energy Harvesting is based on a step-down transformer that regulates the power flow from the piezoelectric element to the desired electronic load. Taking into account parameters of the whole system, the "optimal" voltage gain the piezoelectric transformer can be determined where the harvested power is maximized for the actual level of mechanical excitation. Consequently the piezoelectric transformers can be used to boost up the conversion of mechanical strain into electrical power with considerable potential in Energy Harvesting applications. Nowadays however, the most important factor is usage of lead free material for its construction. Additional desired parameters of such ceramics include high value of piezoelectric coefficients, low dielectric losses and reasonable power density. This work for first time proposes a lead free K$_{0.5}$Na$_{0.5}$NbO$_3$ (KNN) material implementation for stack type of piezoelectric transformer that is designed for load efficiency optimization of vibration energy harvester.

Keywords: Energy Harvesting, Piezoelectric Effect, piezoelectric transformer, piezoelectric properties

1. Introduction

The necessity of battery replacement in electrical power supply of small sensors has directed an interest in energy harvesting, especially in a form, in which electrical energy is captured from a vibrating piezoelectric elements [1]. The top vibration Energy Harvesting applications include helicopters, trains and bearings. In the first case of the helicopter, there is no shortage of vibration available to harvest from during the flight. At the same time many different types of sensors are needed to ensure structural and component health of this flying vehicle. Running wires to all of these sensors is not only complex and costly but also adds weight, which for a helicopter world is at a premium [2].

In the latter case, the vibrations on a train are not as widespread as on helicopters, but they are also strong especially in the truck frame area. Additionally high speed rail solutions create a need for more and more sensors to ensure structural and system health. Wired power is a non-starter due to the amount of wiring needed and the harsh environment under the train [3]. In the United States for example, a project have been completed with the Federal Railway Service (FRA), in which a completely self powered train brake force measurement device was designed, that was able to use a wireless network to communicate the brake force data to the locomotive [4].

In last case of bearing in industrial applications will have hard wire power available, those applications will especially benefit from energy scavenging. However, bearings are typically designed not to have vibration, but bearing vibration is finally an indicator of wear and eventual failure. Consequently, those devices can be designed to harvest from this specific vibration and provide enough energy to alert a condition based maintenance (CBM) system that the bearing needs replacement [5].

So far, the lead zirconate titanate (PZT) ceramics played a dominant role in vibration generators due to their superior piezoelectric properties [6]. Pb-free piezoelectric ceramics have grown in importance through increased environmental reservations to the presence of Pb and the subsequent legislation including directives such as Waste Electrical and Electronic Equipment (WEEE) and the Restriction of Hazardous Substances Directive (RoHS). While much progress has been made on producing Pb-free materials, there are still a number of challenges to increase its performance to effectively form functional devices such as piezoelectric transformer [7].

The criteria for selecting Pb-free piezoelectric ceramic materials for use in piezoelectric transformers are numerous. The main advantages are potassium sodium niobate (KNN)-based piezoceramics have low density, high relative permittivity and mechanical strength in general compared to PZT, especially in the case of textured ceramics [8,9]. Use of some appropriate sintering additive such as CuO is the most economical method to achieve high density and texture in KNN-based ceramics [10]. Another effective way of achieving high density for KNN based compositions is by using non conventional sintering techniques like hot pressing (HP) [11,12]. The motivation in this project is to technologically tailor lead-free material which is comparable to PZT-based ceramics in both performance

*   UNIVERSITY OF SILESIA·INSTITUTE OF TECHNOLOGY AND MECHATRONICS, 12 ŻYTNIA STR.,41-200 SOSNOWIEC, POLAND
** EMPA, SWISS FEDERAL LABORATORIES FOR MATERIALS SCIENCE AND TECHNOLOGY, LABORATORY FOR HIGH PERFORMANCE CERAMICS, 8600 DUEBENDORF, SWITZERLAND
#   Corresponding author: lucjan.kozielski@us.edu.pl, jolanta.dzik@us.edu.pl

and temperature stability. Therefore for the first time, the hot pressed lead-free $K_{0.5}Na_{0.5}NbO_3$ ceramics was obtained and implemented in stacked piezoelectric transformer for energy harvesting application.

2. Experimental

The solid state reaction is desirable for industrial applications and was chosen in this experiment, because it is simple and the absence of a solvent makes the process cost effective. However, due to the moisture sensitivity of the starting raw materials, especially K_2CO_3, the precursors must be dried to maintain stoichiometry.

A more serious and well known problem related to KNN synthesis is the evaporation of alkali oxides formed during decomposition of respective carbonates. The sintering window is very narrow and temperatures should be strictly controlled to achieve a high density without drastic decomposition. Usually implemented methods to get dense stoichiometric KNN compounds are addition of excess alkali carbonates, reducing the powder's particle size and the use sintering aids such as CuO [13-15].

Hot Pressing (HP) is another technique, which can sinter ceramics at lower temperature than conventional solid state reaction making them very attractive for KNN-like materials.

Consequently, for sample preparation the special processing method was used involving drying the K_2CO_3 prior to use in air atmosphere and subsequent milling stoichiometric ratios of K_2CO_3, Na_2CO_3 and Nb_2O_5 according to the $K_{0.5}Na_{0.5}NbO_3$ formula (Sigma Aldrich, 99 % purity). The isopropanol was added to submerge both the reactants and zirconia balls in a planetary mill bowl and then milled for 12 hours to evenly distribute the reagents throughout the powder mix. Later the slurry was dried at 120°C in an oven. Finally the powder was placed in an alumina crucible to synthesize at 950°C for 4 hours.

The synthesised material were crushed and milled again for 12 h to finally achieve reduced average grain size of ~2 μm. The

zirconia balls were removed using steel sieve with deionised water and dried at a temperature of 120°C. At the last stage, polyvinyl alcohol binder about 2% the weight of KNN powder, was added and compacted into cylindrical pellets of 10 mm in diameter and 1 mm in height. The pellets were lastly hot pressed at 20 MPa in alumina matrix for 4 hrs at 1100°C with a 5°C/min ramp rate (R0001 Hot Press, Russia). The sample surfaces were finally wet polished and silver electrodes were deposited on either side of the bulk compact (Electrodag 5915, Acheson Colloids Co. Henkel, Germany).

XRD diffraction patterns were recorded using an XRD PANalyticalX'Pert Pro Multipurpose Diffractometer. The wide-angle scan from 5° to 80° was done with a step width of 0.02° and exposure time of 1250 seconds per step (CuKα-radiation). For phase composition identification of the $K_{0.5}Na_{0.5}NbO_3$ material a quantitative analysis was performed by the Rietveld refinement method based on the respective structural models [16]. The obtained KNN samples microstructure were acquired by JEOL JSM-7100F TTL LVSEM.

Finally, both disks surfaces were coated with Ag epoxy paste (Electrodag 5915, Acheson Colloids Co. Henkel, Germany) to ensure electricalcontact. The dielectric permittivity measurements vs. temperature were carried out on heating by using the QuadTech 7600 Plus Precision LCR Meter (the measuring frequency was equal to 1 kHz). After that all the samples were poled in silicone oil at temperature120°C for 10 min at electric field of 3 kV/mm. The large signal polarization and strain hysteresis as a function of applied electric field wasrecorded at 0.1 Hz (aixACCT System).

3. Results

3.1. Microscopy investigations of the sample surfaces

Figure 1 shows the SEM images of $K_{0.5}Na_{0.5}NbO_3$ samples in two different magnifications. The specimen is composed of large amount of small brick-like grains and small amount of
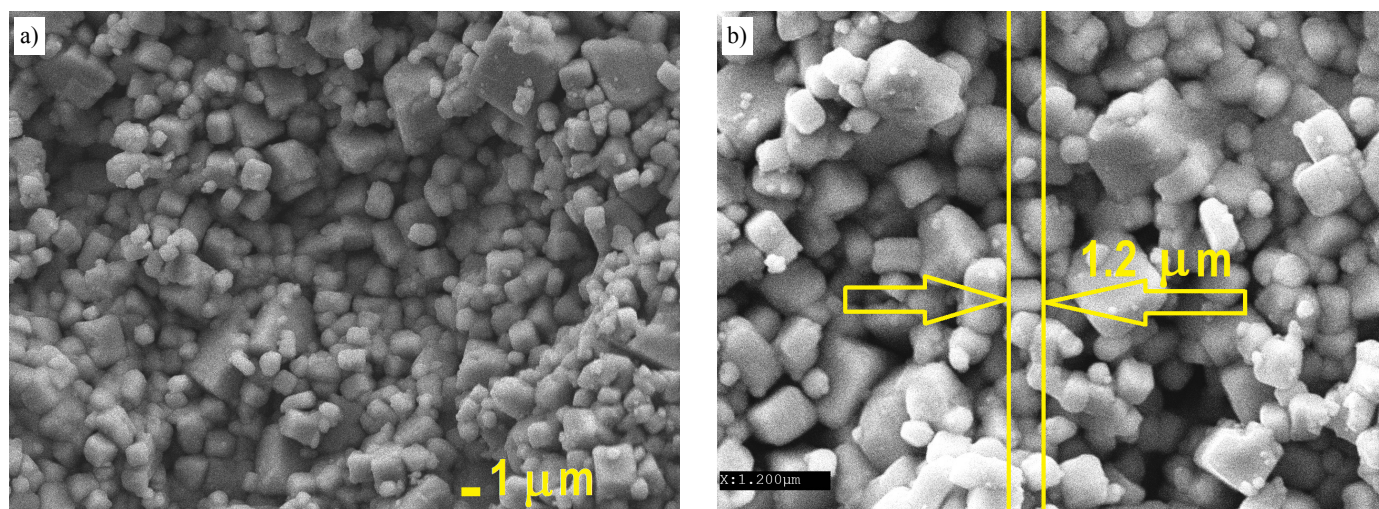

Fig. 1. SEM images of the hot pressed KNN ceramicsin two different magnifications 3000× (a) and 5000× (b)

large rectangular prisms (Fig. 1a). Such a bimodal grain size distribution was also observed in Li- and Sb-substituted KNN ceramics [17,18]. The fracture surfaces of obtained sample are shown by SEM micrographs in Fig. 1b. An investigation reveals that the average grain size of small grains of pure KNN are in the level of 1 micrometer.

3.2. Phase composition identification by X ray diffraction

Figure 2 shows the measured and Rietveld refined XRD diffraction patterns of the $K_{0.5}Na_{0.5}NbO_3$ samples. The crystallographic structure of the KNN unwind from a cubic (C) phase at temperature higher than 400°C to a ferroelectric orthorhombic (O) phase at low temperatures passing through a tetragonal (T) phase. Sometimes the T to O phase transition gives rise to the morphotropic phase boundary area (MPB) with coexistence of both structures that can be located close to room temperature. As a result of the existence of the MPB, excellent piezoelectric properties could be achieved in KNN at room temperature and for this reason KNN is one of the most prospective Pb-free piezoelectric compositions known to date. A report on the pressure-dependent Raman spectra of KNN ceramics indicated that hydrostatic compressive stress favours the orthorhombic phase rather than tetragonal phase [19]. Similarly, the presented Fig. 2 diagram does not show the formation of MPB as it consists only of orthorhombic Amm2 phase. Peak splitting (shown by the arrows) and broadening can be observed in the diffraction patterns clearly indicates that the structure is perovskite with orthorhombic symmetry. Especially the (022) and (200) peaks splitting around 46° with higher value of the (022) peak is an evident confirmation of the orthorhombic lattice. The XRD analysis confirms the formation of all the reflections expected for the Amm2 space group. Although, in general, small amounts of impurities do not significantly affect the pattern but there are some small peaks at 28.8, 43.2 and 49.2 deg (2 theta) so the material is not purely single phased. The XRD analysis indicated them as potassium iron oxides created probably by above mentioned thermal decomposition. The diffraction patterns for KNN, refined to orthorhombic structure with space group Amm2, give lattice parameters $a = 3.957174$, $b = 5.632833$ and $c = 5.649594$ Å.

To determine crystal orientation of the KNN grain a plane of the sample on which X-ray analysis was done, in relation to the pressing force, was chosen. The measurement was done in a way that X-ray radiation was in parallel to the pressing force direction. Consequently, it is distinctly visible higher intensity of (111) reflection, while lower of (100), with respect to the model structure [20]. Such a difference, usually indicate certain
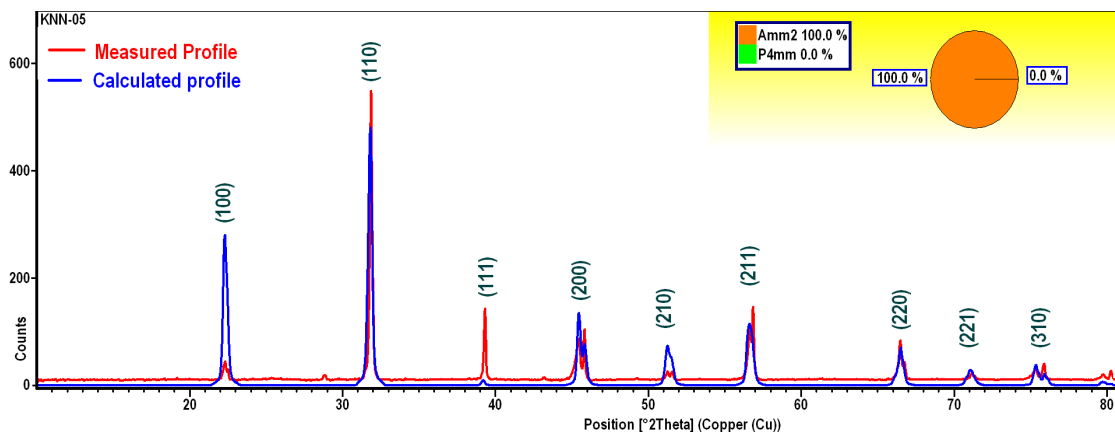

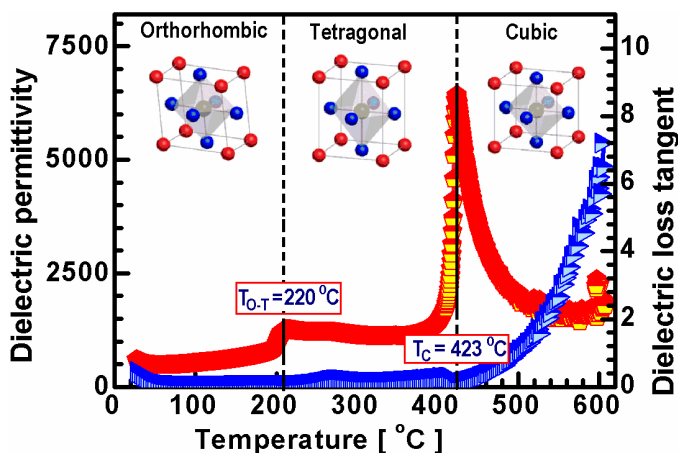Fig. 2. XRD diffraction patterns of obtained $K_{0.5}Na_{0.5}NbO_3$ ceramics

Fig. 3. Dielectric permittivity and dielectric loss tangent temperature KNN dependencies

distortion or preferred orientation of the crystalline structure that will be also reflected later in asymmetric ferroelectric hysteresis.

3.3. Dielectric properties

The complex dielectric permittivity was studied in temperature range from 20 to 600°C and all the phase transitions are presented in Figure 3 (the measuring frequency was equal to 1 kHz). It is confirmed that the crystallographic structure of the KNN evolves from a cubic (C) phase at temperature 423°C to a ferroelectric orthorhombic (O) phase at 220°C passing through a tetragonal (T) phase. Dielectric loss tangent δ value is also reasonable and is not higher than 0,5 in whole functional temperature range (below the Curie Temperature at 423°C).

3.4. Ferroelectric properties

The polarization-electric field behavior of obtained KNN material is shown in Figure 4a. Interesting property is that well saturated hysteresis curve could be obtained only in positive electric field direction. For the negative polarity of electric field, not as much ferroelectric domain can be reoriented, as in opposite direction so that the remnant polarization values are different ($P_{r+} \sim 5.34 \ \mu C/cm^2$ while $P_{r-} \sim 3.26 \ \mu C/cm^2$). Such a behavior is probably caused by preferred crystallographic orientation of grains in the ceramic (111 direction) due to the fact that polarization direction is in the same direction as the preferable crystallographic grain orientation. Similarly asymmetric uniaxial displacement was recorded during piezoelectric coefficients measurements in obtained KNN material ($D_+ = 0.04$ while $D_- = 0.12\%$ at electric field of ± 20 kV/cm) (Fig. 4b). After identification of structural distortion during XRD measurements in KNN sample, there is no surprise that the P-E loop presents the asymmetric shape as expected for ceramics with preferred orientation direction. Different displacements respectively recorded, also confirms variant piezoelectric behavior for alternating electric field.

KNN ferroelectric ceramics made by simple solid state reaction were also reported to exhibit asymmetrical polarization hysteresis loops. This effect is usually associated with an internal bias field connected to the creation of defect dipoles, by pairs of acceptor ions and oxygen vacancies that results in domain wall motion pinning [21].

The authors are convinced that this P-E loops asymmetry is also a consequence of building up of the internal bias field. However the reasons of creation of an internal bias are different, but the asymmetry occurrence is based on the same stabilization of domain wall movement. In uniaxial hot pressed KNN material, the grains crystallographic orientation, preferentially align themselves along the applied pressure axis (Fig. 2). Finally there was experimentally revealed that this internal bias field is stabilizing the polarization and pinning, and/or clamping the domain wall motion. Similar space charge effect, that locking the ferroelectric domains, were frequently reported in thin films, due to the clamping effect of substrate [22].

3.5. Piezoelectric coefficients evaluation

The recorded extreme values of impedance modulus and phase, for the first and second resonant frequency, are presented at Figure 5 a and b, respectively. The calculated piezoelectric parameters of the homogeneous KNN discs were measured according to the standard method (EN 50324-2) [23] and listed in Table 1.

The asymmetric ferroelectric properties are reflected additionally in directional variant values of dielectric permittivity as well as in significantly different values of transversal and longitudinal piezoelectric coefficients (Table 1). Interesting fact is that hot pressed KNN material exhibits non zero spontaneous polarization before poling process. Consequently, after polarizing process the recorded polarization in 33 direction has a reasonable value of $d_{33} = 95$ [pC/N], for KNN ceramics, whereas in direction 31 as low as 18. The transversal coupling factor after poling is similarly very low, $k_{31} = 01$ [pC/N].

TABLE 1

Piezoelectric parameters value of the obtained KNN sample

| Parameter	Definition	Value	Unity
ε_r	Dielectric constant	278	[-]
ε_{33}^T	Longitudinal permittivity at constant stress T	2436	[F/m]
d_{33}	Longitudinal piezoelectric coefficient before poling	30	[pC/N]
d_{33}	Longitudinal piezoelectric coefficient after poling	95	[pC/N]
d_{31}	Transversal piezoelectric coefficientafter poling	18	[pC/N]
k_{31}	Transversal coupling factorafter poling	0,1	[-]

a)

b)
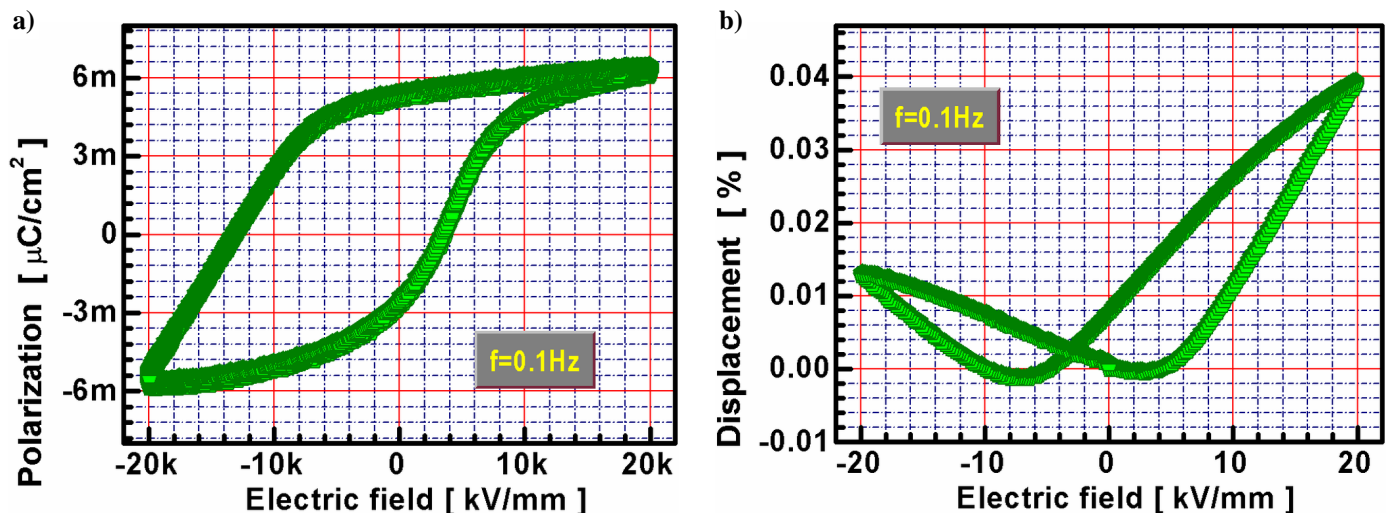
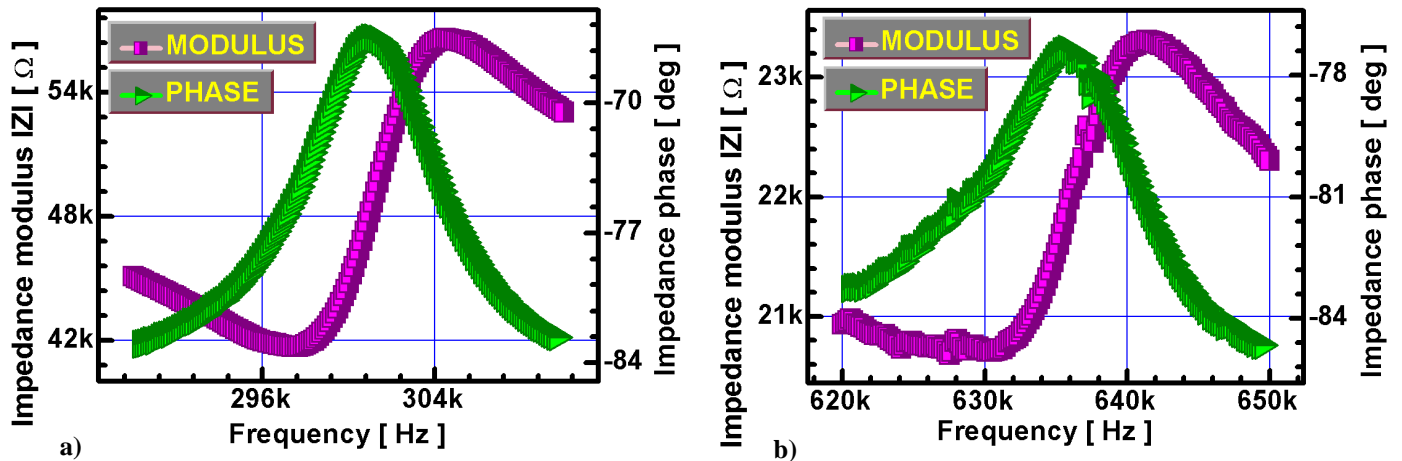Fig. 4. KNN ceramics hysteresis loop (a) and field-induced displacement (b)

Fig. 5. The recorded extreme values of impedance modulus and phase, for first (a) and second (b) resonant frequency

As seen from the presented results, KNN piezoelectric materials show are reasonable promise to replace PZT due to their relatively high piezoelectric properties and high Curie temperature. Since, KNN is currently limited by manufacturing issues, it would be fitting for applications in future designs rather than immediate modification.

3.6. Piezoelectric transformer characteristics

Finally the two KNN discs were stacked, glued and wired for the piezoelectric transformer (PT) characteristics evaluation. The recorded data of gain (a) and efficiency (b) vs. variant load ($R_L \approx 1 - 100$ kΩ) are shown in Fig. 6. It is clearly seen, that the theoretical expectation about strong dependence of output voltage to the load resistance in the lead free ceramic is confirmed. The voltage gain is significantly increasing with rising resistance and the highest recorded value is equal 0.19 for the 100 kW at the resonant frequency of 271 kHz (see Fig. 6a). This rule is not further supported by the measured efficiency for the PT, when

only at low load conditions is this value maximal and close to $eff = 3.4\%$ (see Fig. 6b). Valuable property from the application point of view is that lower than resonant frequency efficiency characteristic has its optimal load value equal $R_L = 10$ kW at frequency of 181 kHz ($eff = 4.8\%$).

4. Conclusions

Uniaxial hot pressing method was successfully implemented for structurally oriented $K_{0.5}Na_{0.5}NbO_3$ ceramics processing. Dielectric measurements revealed that the crystallographic structure of the obtained KNN evolves from a cubic (C) phase at temperature 423°C to a ferroelectric orthorhombic (O) phase at 220°C passing through a tetragonal (T) phase.

As a consequence of grains preferred crystallographic 111 direction, the obtained material exhibits non zero value of spontaneous polarization and additionally has strong asymmetrical ferroelectric hysteresis loop. Finally, also longitudinal piezoelectric coefficients were much higher than transversal, so that the best configuration of piezoelectric transformer for
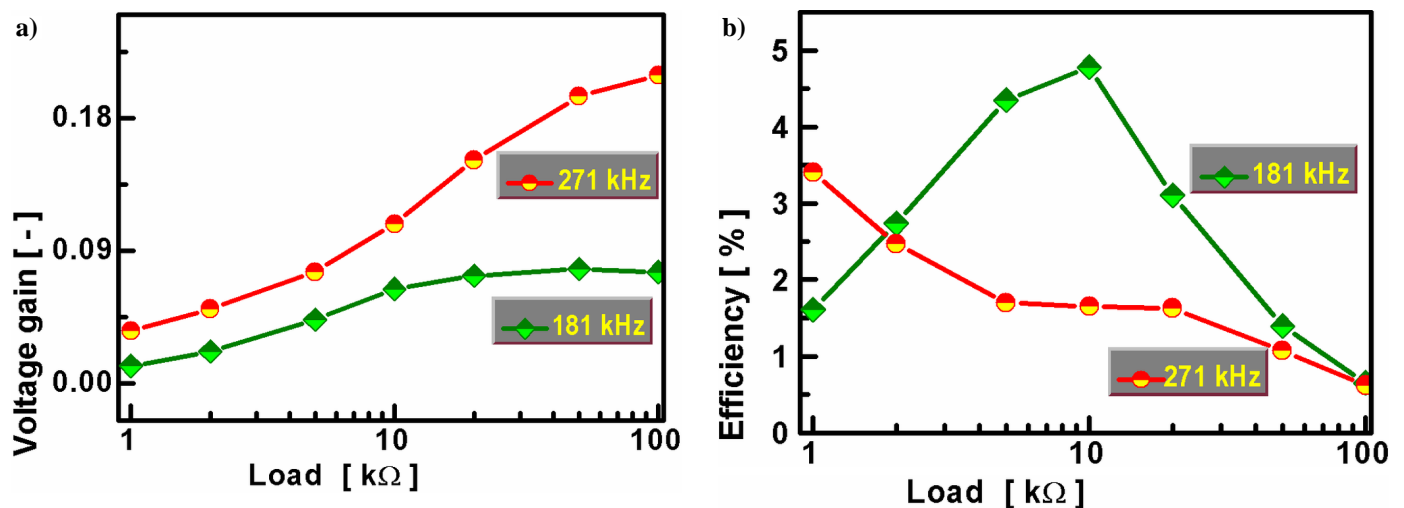

Fig. 6. The experimental data of gain (a) and efficiency (b) vs. various load condition ($Z_L \approx 1 - 100$ kΩ) for the stacked KNN transformer

this particular ceramics is the stacked one. In this case, we can get performance comparable with Piezoelectric Transformers made from lead contained ceramics (PZT "Navy I" Piezoelectric Charge Constant d_{33} = 290 10^{-12} C/N).

As expected, a strong dependence of output voltage of the lead-free piezoelectric transformer to the load resistance was recorded. The most valuable property from the application point of view is, that lower than resonant frequency efficiency characteristics have its optimal load value higher than from resonant frequency.

REFERENCES

[1] A. Erturk, D.J. Inman, Piezoelectric Energy Harvesting, John Wiley & Sons (2011).

[2] S.W. Arms, C.P. Townsend, D.L. Churchill, S.M. Moon, N. Phan, Energy Harvesting Wireless Sensors for Helicopter Damage Tracking, Proceedings of AHS International Forum 62, HUMS III session, Phoenix, AZ, pp. 1-6 (2006).

[3] S.M. Rakshit, M. Hempel, P. Shrestha, F. Rezaei, H. Sharif, J. Punwani, M. Stewart, Energy Analysis in Deploying Wireless Sensor Networks for On-Board Real-Time Railcar Status Monitoring, 2015 Joint Rail Conference San Jose, California, USA, Paper No. JRC2015-5765, pp. V001T03A005-14 (2015).

[4] S. Saadat, C. Stuart, G. Carr, J. Payne, 2014 Joint Rail Conference Colorado Springs, Colorado, USA, Paper No. JRC2014-3860, pp. V001T05A002-7 (2014).

[5] R. Torah, P. Glynne-Jones, M. Tudor, T. O'Donnell, S. Roy, S. Beeby, Meas. Sci. Technol. **19**, 125202-125210 (2008).

[6] W. Heywang, K. Lubitz, W. Wersing, Piezoelectricity: evolution and future of a technology, Springer Science & Business Media (2008).

[7] S. Priya, D.J. Inman, Energy Harvesting Technologies, Springer US (2009).

[8] M. Ichiki, L. Zhang, M. Tanaka, R. Maeda, J. Europ. Ceram. Soc. **24**, 1693-1697 (2004).

[9] M. Demartin-Maeder, D. Damjanovic, N. Setter, J. Electroceram. **13**, 385-392 (2004).

[10] D. Lin, K.W. Kwok, H.L.W. Chan, J. Appl. Phys. **102**, 074113 (2007).

[11] X. Duan, D. Jia, Z. Wu, Z. Tian, Z. Yang, S. Wang, Y. Zhou, Scripta Mater. **68**, 104-107 (2013).

[12] M. Adamczyk, L. Kozielski, M. Pawełczyk, Ceram. Int. **34**, 1617-1622 (2008).

[13] R. Zuo, J. Roodel, R. Chen, L. Li, J. Am. Ceram. Soc. **89**, 2010-2015 (2006).

[14] K. Wang, J.-F. Li, J. Am. Ceram. Soc. **93**, 1101-1107 (2010).

[15] I.T. Seo, K.H. Cho, H.Y. Park, S.J. Park, M.K. Choi, S. Nahm, H.G. Lee, H.W. Kang, H.J. Lee, J. Am. Ceram. Soc. **91**, 3955-3960(2008).

[16] H.M. Rietveld, J. Appl. Crystallogr. **2**, 65-71 (1969).

[17] R. Gaur, K.C. Singh, R. Laishram, Ceram. Int. **41**, 1413-1420 (2015).

[18] H.E. Mgbemere, G.A. Schneider, Funct. Mater. Lett. **25**, 1-9 (2010).

[19] K. Kakimoto, T. Sumi, I. Kagomiya, Jpn J. Appl. Phys. **49**, 09DM10 (2010).

[20] B. Orayech, A. Faik, G.A. López, O. Fabelo, J.M. Igartua, J. Appl. Crystallogr. **48**, 1-16 (2015).

[21] S. Zhang, J.B. Lim, H.J. Lee, T.R. Shrout, IEEE Trans. Ultrason. Ferroelectr. Freq. Control. **56** (8), 1523-1527 (2009).

[22] L. Pintiliea, M.I. Vrejoiu, G. Le Rhun, M. Alexe, J. Appl. Phys. **101**, 064109 (2007).

[23] IRE Standards on Piezoelectric Crystals: Measurement on Piezoelectric Ceramics IEEE, New York (1961).